

Modeling of vapour absorption refrigeration system assisted by solar photovoltaic and electrolyzer-polymer electrolyte membrane fuel cell

Dr. Kamaljyoti Talukdar¹

¹Assistant Professor, Department of Mechanical Engineering, Bineswar Brahma Engineering College, Kokrajhar-783370, Assam, India

Abstract: In the present paper, power is supplied to the generator of vapour absorption refrigeration system(VARS) in Kolkata city, India. During day time power required in the generator of an absorption refrigeration system is obtained from sunlight falling on solar photovoltaic(SPV) modules and extra current after meeting the requirements of the generator is sent to electrolyzer where water present in electrolyzer is dissociated into hydrogen and oxygen. The hydrogen produced having high volume is sent to a gas compressor for compression and stored in a small volume tank with the help of power obtained from separate solar photovoltaic modules. During night time hydrogen stored in tank is utilized by polymer electrolyte membrane(PEM) fuel cell thereby supplying power to the generator. The study reveals that 1213 solar photovoltaic modules in parallel each having 2 modules in series of Central Electronics Limited Make PM 150 with a 246.258 kW electrolyzer and 36 PEM fuel cell stacks, each of 382.372 W, can support the energy requirement of the generator of water-LiBr absorption refrigeration system of 10 TOR(ton of refrigeration) and for gas compressor 125 solar photovoltaic modules in parallel each having 2 modules in series of Central Electronics Limited Make PM 150 is needed.

Keywords - Central Electronics Limited Make PM 150, Electrolyzer, Polymer electrolyte membrane(PEM), Solar photovoltaic(SPV), Water-LiBr.

Date of Submission: 21-06-2020

Date of Acceptance: 10-07-2020

I. INTRODUCTION

Due to increased pollution, ozone hole depleting substances and release of global warming potential gases, research is going to reduce these polluting gases and global warming gases. At present vapour compression refrigeration systems are used abundantly which releases a lot of ozone-depleting gases from the refrigerants used. Although alternative refrigerants are used still some amount of pollution occurs to some degree. The use of vapour compression refrigeration system needs a great amount of electrical energy to operate along with the sound problem in a compressor. Hence research is going on to use alternative refrigeration systems like vapour absorption refrigeration system which uses power or waste heat to operate.

The present paper deals with the use of power obtained from a combined solar photovoltaic system and electrolyzer-polymer electrolyte membrane fuel cell to operate an absorption refrigeration system. Many works related to fuel cell and photovoltaic modules have been done by researchers. Wu et al [1] presented an integrated framework for fuel cell-based distributed energy applications. Yildiz et al [2] developed and tested to investigate the exergetic performance of a solar photovoltaic system (PV) assisted earth-to-air heat exchanger (underground air tunnel) that is used for greenhouse cooling at the Solar Energy Institute, Ege University, Izmir, Turkey. Bai et al [3] focused on an experimental and numerical study of the behavior of a PV-SDHW(photovoltaic- solar domestic hot water) system, focusing on the start-up phase optimized through various electronic devices. A detailed model of a circulation pump was developed by considering a direct current (DC) circulation pump coupled with various electronic devices (linear current booster and maximum power point tracker). The developed models were then validated experimentally, to reveal the influence of the threshold solar radiation on the circulation pump start-up and the pump flow rate as a function of the solar radiation, and its effects on the annual energy performance of PV-SDHW systems. Kelly et al [4] determined the efficiency and other operational characteristics of the PV(photovoltaic)-ESD(electrolyzer/storage/dispensing)system during testing over 109 days at the GM Proving Ground in Milford, MI, at a hydrogen output pressure of approximately 2000 psi (13.8 MPa). Solis et al [5] proposed a new approach for H₂ production by PEM electrolysis, assisted by effluent treatment in the anolyte. Dorer et al [6] presented a methodology for assessing the performance of small combined heat and power (micro-cogeneration) systems in terms of primary energy demand and the CO₂ emissions by transient computer simulations was established, and demonstrated for a natural gas-driven solid

oxide fuel cell (SOFC) and, to a lesser extent, a polymer electrolyte fuel cell (PEFC) home fuel cell cogeneration system. Tributsch [7] addressed the criticality of photovoltaic hydrogen generation and made a review on the required innovative technology for the conversion of light into electricity. Also, strategies were aimed at either decentralizing photovoltaic hydrogen generation or centralizing it in specialized power plants and are compared and their respective potential evaluated. Jie et al [8] proposed a novel heat pump system in which PV/T(photovoltaic.thermal) collector is coupled with a solar-assisted heat pump and works as an evaporator. Hawkes et al [9] analyzed the potential of the technology, a detailed techno-economic energy-cost minimization model of a micro-CHP(combined heat and power) system was developed drawing on steady-state and dynamic SOFC stack models and power converter design. This model was applied to identify minimum costs and optimum stack capacities under various current density change constraints.

The present paper will discuss the performance characteristics of a combined solar photovoltaic system and electrolyzer-polymer electrolyte membrane fuel cell to operate an absorption refrigeration system.

II. SCHEMATIC LAYOUT OF COMBINED SYSTEM

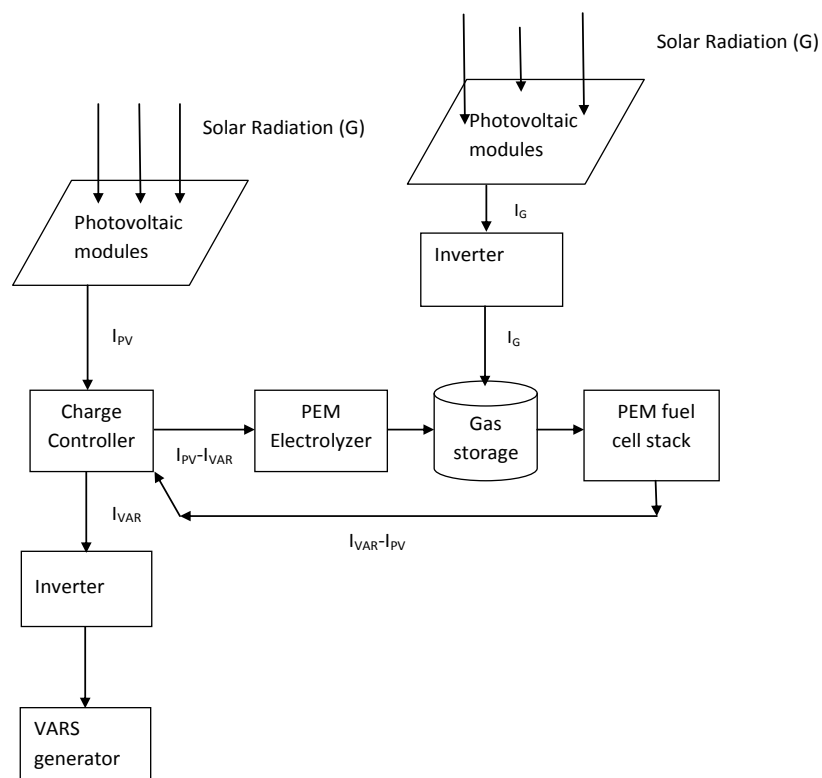


Fig.1: Schematic view of combined solar photovoltaic-electrolyzer polymer electrolyte membrane fuel cell to supply power to generator of VARS

Fig.1 shows a brief layout of the proposed system. For powering VARS' generator power is obtained in different layout during daylight and night time. During the daytime, solar radiation falls on solar photovoltaic modules and generates direct current (I_{PV}). It is sent through a charge controller. In the charge controller, the required current is sent to the VARS generator(I_{VAR}) after passing through an inverter. The remaining excess current($I_{PV}-I_{VAR}$) is sent to the electrolyzer. In electrolyzer, the water present is dissociated into hydrogen and oxygen. Hydrogen having low mass density needs a large tank for storage. Hence to reduce the storage tank size hydrogen is compressed which obtains its power(I_G) again from solar photovoltaic modules.

During night time when radiation is not available, the PEM fuel cell stack uses stored hydrogen from the storage tank and generates a current ($I_{VAR}-I_{PV}$) and is sent to the VARS generator through a charge controller.

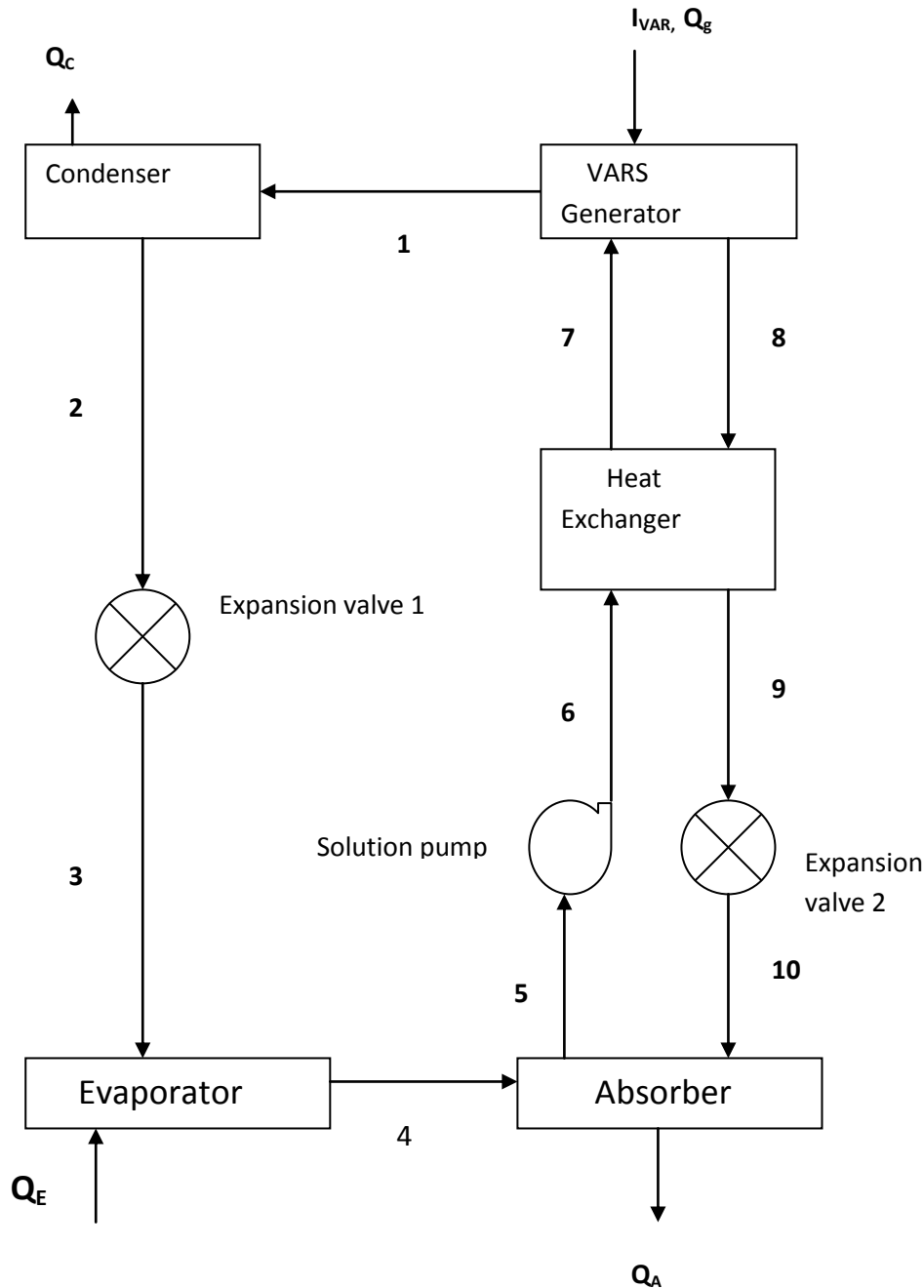


Fig 2: Schematic view of water-LiBr VARS

Fig. 2 shows a schematic of water-LiBr VARS, where water is the refrigerant and LiBr is the absorbent. Water coming from state 3 enters the evaporator. In the evaporator, water absorbs cooling load Q_E from the required space and converts into saturated vapour at state 4. Refrigerant water enters the absorber and mixes with LiBr to form a strong solution that is pumped to the generator via heat exchanger by solution pump through path 5-6-7. Due to the mixing of water and LiBr in absorber heat (Q_A) is generated which is rejected to ambient. In generator heating of a strong solution coming from the absorber is done by power coming from the charge controller as mentioned in fig.1. The water having a lower boiling point than LiBr some amount of water evaporates and goes to the condenser. The remaining solution formed is weak and is sent to absorber through path 8-9-10 after passing through the heat exchanger and expansion valve 2. The water in vapour form rejects heat (Q_C) and converts into saturated liquid. This saturated liquid is sent to the evaporator after passing through expansion valve 1 and the cycle continues.

III. MODELING

Modeling of VARS

Mass flow rate of refrigerant (m_{H_2O}) is :

$$m_{H_2O} = \frac{Q_E}{h_4 - h_3} \quad (1)$$

Where, Q_E is cooling load(kW), h_4 , h_3 enthalpy(kJ/kg) at state 4 and 3 respectively.

Concentration of strong solution(X_{ss}) is given from [10]:

$$X_{ss} = \frac{49.04 + 1.125T_A - T_E}{134.65 + .47T_A} \quad (2)$$

Concentration of weak solution(X_{ws}) is given from [10]:

$$X_{ws} = \frac{49.04 + 1.125T_G - T_C}{134.65 + .47T_G} \quad (3)$$

Where T_A , T_E , T_G , T_C are temperatures of absorber, evaporator, generator, condenser respectively.

Mass flow rate of strong solution (m_{ss}) [10]:

$$m_{ss} = \frac{m_{H_2O} \times X_{ws}}{X_{ws} - X_{ss}} \quad (4)$$

Where, X_{ws} -concentration of weak solution, X_{ss} -concentration of strong solution.

Mass flow rate of weak solution (m_{ws}) [10]:

$$m_{ws} = \frac{m_{H_2O} \times X_{ss}}{X_{ws} - X_{ss}} \quad (5)$$

Generator heat load(Q_g) is given by:

$$Q_g = m_{H_2O} \times h_1 + m_{ws} \times h_8 - m_{ss} \times h_7 \quad (6)$$

Where, h_1 , h_8 and h_7 are enthalpy(kJ/kg) at states 1, 8 and 7 respectively.

Thermodynamic properties such as specific enthalpy of the refrigerant (water) both in liquid and vapour state at various pressures and temperatures are determined from International Associations for the properties of water and steam (IAPWS) formulation 1997 [11]. Similarly, the thermodynamic properties of H_2O -LiBr solutions at various temperatures and concentrations are calculated using the correlations proposed by Patek and Klomfar [12].

Modeling of solar photovoltaic system

The modules used for the analysis are taken from [13] and detailed calculation for solar photovoltaic (SPV) is obtained from [14]. Also, solar radiation, ambient temperature, and wind speed data of Kolkata city for SPV calculations are obtained from references given in [14].

The number of modules connected in series (N_s) of the entire photovoltaic array [14] is:

$$N_s = \frac{V_{system}}{V_{module}} \quad (7)$$

Where, V_{system} - system voltage of the photovoltaic array(48V), V_{module} -voltage obtained from single module [13].

The hourly current($i_{i,VARS}$) required to give power to generator is given by:

$$i_{i,VARs} = \frac{Q_g}{V_{system} \times PF \times \eta_{inverter}} \quad (8)$$

Where, Q_g -hourly generator heat load, PF-power factor(considered 0.85), $\eta_{inverter}$ -inverter efficiency(0.85 considered).

The total current required to power generator(i_{total}) throughout a day:

$$i_{total} = \sum i_{i,VARs} \quad (9)$$

Where, $\sum i_{i,VARs}$ -summation of hourly current,

The design current(i_{spv}) required from solar photovoltaic modules is similar to given by [14]:

$$i_{spv} = \frac{i_{total} \times DF}{sunshinehours \times \eta_{chargecontroller}} \quad (10)$$

Where, DF-derating factor of photovoltaic modules [15], $\eta_{chargecontroller}$ -charge controller efficiency (0.85)[15],sunshine hours considered 7 for Kolkata city [16].

The number of photovoltaic modules in parallel (N_p) is given by [14]:

$$N_p = \frac{i_{spv}}{i_{mp}} \quad (11)$$

Where i_{mp} -maximum current by photovoltaic module [13]

Current generated by combined modules (I_{PV}) is given by:

$$I_{PV} = i_{pv} \times N_p \quad (12)$$

Where i_{pv} -current generated by single module.

Modeling of PEM fuel cell

All the input parameters and calculations for finding net voltage are obtained from [14].

The peak hourly current required from fuel cell stack ($i_{fuelcell,VAR}$) is given by:

$$i_{fuelcell,VAR} = \frac{peakgeneratorcurrent}{\eta_{chargecontroller}} \quad (13)$$

Where, peak generator current is the maximum current requirement at any hour during non sunshine hours i.e. from 1:00 hour to 5:00 hours and 19:00hours to 24:00 hours.

Number of PEM fuel cell stacks in parallel($N_{fc,parallel}$) is given by [14]:

$$N_{fc,parallel} = \frac{i_{fuelcell,VAR}}{i_{cell}} \quad (14)$$

Where i_{cell} -current generated by single fuel cell.

The number of fuel cell connected in series($N_{fc,series}$) and is given by[14]:

$$N_{fc,series} = \frac{V_{system,fc}}{V_{fc}} \quad (15)$$

Where $V_{system,fc}$ -system voltage of fuel cell(48V considered), V_{fc} -net voltage of PEM fuel cell.

The hourly hydrogen consumption of a fuel cell stack during non sunshine hours is given from [14]:

$$m_{fc,VAR} = \frac{i_{fuelcell,VAR} \times N_{fc,series} \times 3600 \times 2}{2 \times F \times \eta_{fuel}} \quad (16)$$

Where F is Faraday constant (96500 C/mole), η_{fuel} -fuel utilization factor in fuel cell (considered 0.9)

Modeling of PEM electrolyzer

Excess current ($I_{PV}-I_{VAR}$) after meeting the requirement of the generator heat load is sent to the PEM electrolyzer for dissociating water present in electrolyzer into oxygen and hydrogen. The number of cells in stack in series is taken as 30 and effective cell area is considered to be 86.4 cm² [17].

Amount of hydrogen produced(in gram mol)in electrolyzer with 30 cells in series in hourly basis is given by [14]:

$$M_{elec,VAR} = \frac{(I_{PV} - I_{VAR}) \times 30 \times \eta_{elec} \times 3600}{2 \times F} \quad (17)$$

Where, η_{elec} -electrolyzer electrical efficiency, I_{VAR} - hourly current requirement from PV modules(6:00 hours to 18:00 hours)

Modeling of gas compressor

Hydrogen gas produced in the electrolyzer needs to be compressed to store it in less volume which is obtained from a separate system of a solar photovoltaic system. The required input parameter for power calculation in the gas compressor is obtained from [14].

Current required for running the gas compressor at i_{th} hour in a day is given by :

$$i_{compressor,i} = \frac{W_{c,i}}{V_{system,compressor} \times PF \times \eta_{inverter}} \quad (18)$$

Where $V_{system,compressor}$ - system voltage of compressor(48 V considered), $W_{c,i}$ - power required to run the gas compressor in hourly basis(6:00 -18:00 hours, sunshine hours).

Total current required by gas compressor is :

$$i_{compressor,total} = \sum_{i=6}^{18} i_{compressor,i} \quad (19)$$

The design current($i_{spv,c}$) required from solar photovoltaic modules is similar to given by [14]:

$$i_{spv,c} = \frac{i_{compressor,total} \times DF}{sunshinehours \times \eta_{chargecontroller}} \quad (20)$$

The number of photovoltaic modules in parallel (N_p) is given by [14]:

$$N_p = \frac{i_{spv,c}}{i_{mp}} \tag{21}$$

IV. RESULTS AND DISCUSSIONS

Table 1: Temperatures of various components of VARS

Components	Temperature
Evaporator(T _E)	15 ⁰ C
Absorber(T _A)	Ambient temperature of Kolkata city, India(May and December)
Generator(T _G)	80 ⁰ C
Condenser(T _C)	Ambient temperature of Kolkata city, India(May and December)

The heat exchanger effectiveness of VARS is considered 0.8. Fig. 3 shows the variation of the mass flow rate of the strong solution and weak solution for May and December for the water-LiBr vapour absorption refrigeration system.

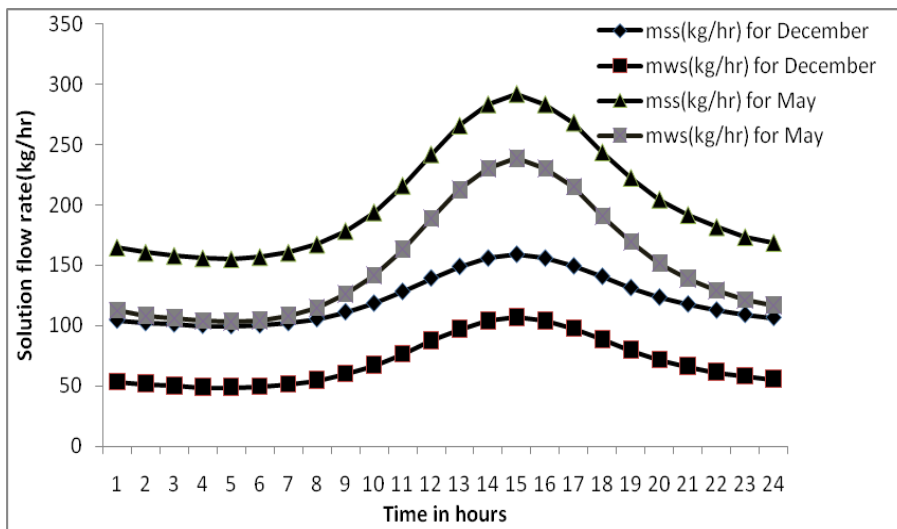


Fig.3: Variation of mass flow rate of strong and weak solution of water-LiBr absorption refrigeration system

It is seen that the mass flow rate of the strong solution decreases from 1:00 hour to 5:00 hours because the concentration of weak solution increases due to decrease in temperature of condenser and concentration of strong solution decreases as absorber temperature decreases and due to more dominance of absorber temperature in numerator than the denominator. But the effect of the increase in (X_{ws}-X_{ss}) in the denominator is more dominant than X_{ws} increase in numerator according to equation no. 4. From 6:00 hours to 15:00 hours mass flow rate of the strong solution increases since the concentration of weak solution decreases due to an increase in temperature of condenser and concentration of strong solution increases as absorber temperature increases and due to more dominance of absorber temperature in numerator than the denominator. But the effect of the decrease in (X_{ws}-X_{ss}) in the denominator is more dominant than X_{ws} decrease in the numerator. Again mass flow

rate of the strong solution decreases from 16:00 hours to 24:00 hours due to the same reason mentioned for 1:00 hour to 5:00 hours as ambient temperature again decreases from 16:00 hours to 24:00 hours.

It is seen that the mass flow rate of the weak solution decreases from 1:00 hour to 5:00 hours since the concentration of strong solution decreases due to a decrease in temperature of absorber and concentration of weak solution increases due to a decrease in condenser temperature. But the effect of the increase in $(X_{ws}-X_{ss})$ in denominator and X_{ss} decrease in numerator lead to these variations according to equation no. 5. The mass flow rate of the weak solution increases from 6:00 hours to 15:00 hours since the concentration of the strong solution increases due to an increase in absorber temperature and concentration of weak solution decreases due to an increase in condenser temperature. But the effect of the decrease in $(X_{ws}-X_{ss})$ in denominator and X_{ss} increase in numerator leads to this variation. Again mass flow rate of the weak solution decreases from 16:00 hours to 24:00 hours due to the same reason mentioned for 1:00 hour to 5:00 hours as ambient temperature again decreases from 16:00 hours to 24:00 hours.

The mass flow rate of the strong solution and weak solution is more in May than December due to greater ambient temperature (for condenser and absorber) in May than December and the concentration of strong and weak solution changes accordingly as mentioned previously.

Fig. 4 shows variation of generator heat load for the month of May and December.

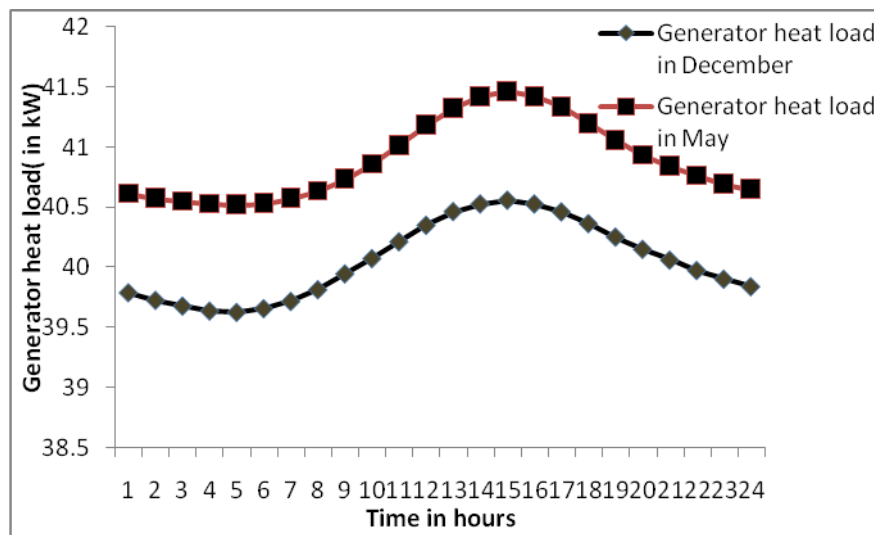


Fig. 4: Variation of generator heat load in the month of May and December

The variation of generator heat load (Q_g) can be explained by equation 6. The mass flow rate of refrigerant (m_{H2O}) and enthalpy h_1 remains the same, since cooling load and evaporator temperature remain constant i.e. 10 TOR and 15°C respectively. Enthalpy at point 8 (h_8) remains the same since the generator temperature is constant (80°C). However, enthalpy at 7 (h_7) changes accordingly as absorber temperature (ambient temperature) changes from 1:00hour to 24:00 hours in a day. Also, the mass flow rate of weak and strong solution changes in the pattern shown in figure 3. Hence generator heating load also follows the same trend as that shown in figure 3.

Generator heating load is more in May than December as h_7 is more due to greater absorber temperature in May. Also, the mass flow rate of a strong and weak solution is more in May as explained in figure 3.

The number of photovoltaic modules needed in series (which is 2) obtained from equation no. 7, where V_{system} is 48 V and V_{module} is 34 V [12]. The hourly current requirement for VARS generator ($i_{i,VARS}$) is obtained from equation 8 and varies in the same trend as Q_g varies in a day. It is seen that for December $i_{i,VARS}$ decreases from 1:hour (1147.332 A) to 5:00 hours (1142.641 A); increases from 6:00 hours (1143.540 A) to 15:00 hours (1169.428 A) and again decreases from 16:00hours (1168.557 A) to 24:00 hours (1148.777 A). The hourly current required from solar photovoltaic modules for VARS generator (I_{VAR}) is obtained by equation 10 by substituting $i_{i,VARS}$ in place of i_{total} for December and May. It is seen that for December hourly current requirement from PV modules decreases from 1:00hour (241.036 A) to 5:00 hours (240.051 A); increases from

6:00 hours (240.239 A) to 15:00 hours(245.678 A) and again decreases from 16:00hours(245.495 A) to 24:00 hours (241.339 A). It is seen that for May $i_{i,VARs}$ decreases from 1:00hour(1170.992 A) to 5:00 hours(1168.342 A);increases from 6:00 hours (1168.773 A) to 15:00 hours(1195.532 A) and again decreases from 16:00hours(1194.236 A) to 24:00 hours (1172.143 A). It is seen that for May hourly current requirement from PV modules decreases from 1:00hour(246.006 A) to 5:00 hours(245.450 A);increases from 6:00 hours (245.540 A) to 15:00 hours(251.162 A) and again decreases from 16:00hours(250.890 A) to 24:00 hours (246.248 A). By equation 9, the summation of all hourly generator current (i_{total}) in a day is done and by putting the i_{total} in equation 10 for December, i_{spv} for December is obtained. Also, i_{spv} can be obtained by summing all the hourly current requirements from PV modules(I_{VAR}). By using equation 11 and i_{mp} as 4.8 A[13], the number of solar photovoltaic modules in parallel(N_p) obtained is 1213. For calculating N_p , i_{total} of December is considered as month December has minimum solar radiation and if module numbers are satisfied in December, the system will work throughout the year.

The peak hourly current required from fuel cell stack ($i_{fuelcell,VAR}$) is obtained from equation 13, where peak generator current during non-sunshine hours $i_{i,VARs}$ and current required from PV modules(I_{VAR}) occurs at 19:00 hours (1160.621 A, 243.828 A for December respectively) and 1183.854 A, 248.708 A for May respectively. The number of fuel cells in parallel is found to be 36 by dividing $i_{fuelcell,VAR}$ by 7.966 A(current generated by single fuel cell[14]). The number of fuel cells in series ($N_{fc, series}$) is obtained by dividing 48(system voltage of fuel cell) by the net voltage of a single fuel cell(1.028 V) and is found to be 47. The maximum current output of each fuel cell stack in series is 7.966 A and the power of each fuel cell stack is given by-product of 48 V and 7.966 A which is 382.372 W.

In electrolyzer number of cells in series is considered to be 30.

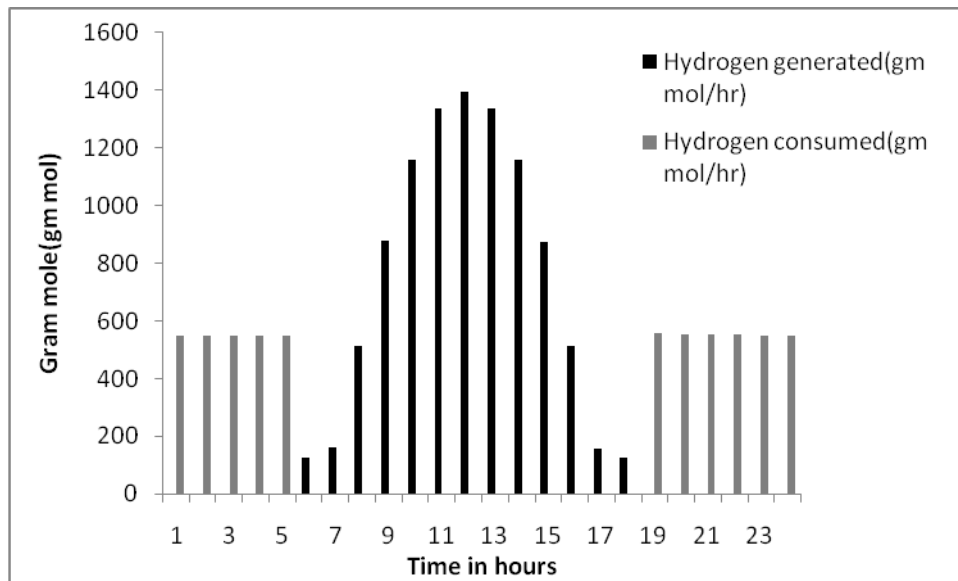


Fig. 5: Variation of hourly hydrogen consumption and hydrogen generation for December

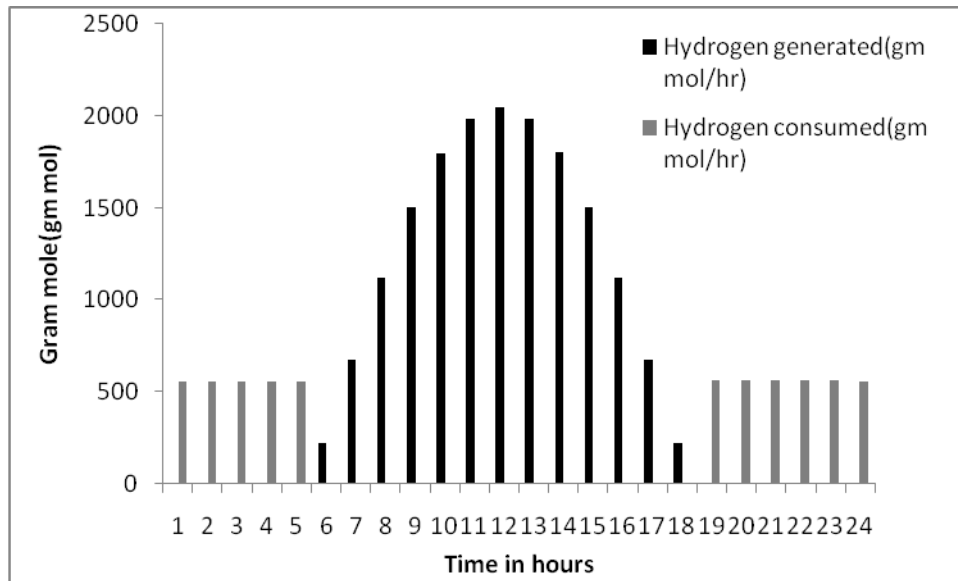


Fig. 6: Variation of hourly hydrogen consumption and hydrogen generation for May

Figure 5 and 6 shows hydrogen consumption and generation for December and May. It is seen that hydrogen consumption by fuel cell decreases from 1:00 hour to 5:00 hours and also from 19:00 hours to 24:00 hours due to a decrease in hourly generator heating load (Q_g) and thereby decreasing hourly generator current. It is seen that hourly hydrogen generation by electrolyzer increases from 6:00 hours to noon and again decreases to 18:00 hours because solar radiation increases from 6:00 hours to noon and again decreases to 18:00 hours. As a result, the term I_{PV} increases proportionally from 6:00 hours to noon and again decreases to 18:00 hours. Although I_{VAR} (generator current) changes according to the trend shown in figure 4, the change of I_{PV} is more dominant than the change in I_{VAR} as can be seen in equation 17.

It is also seen that hydrogen consumption in May is more than December due to the greater amount of hourly generator current in May. Also, hydrogen generation is more in May than December due to a greater amount of solar radiation availability.

The cumulative hydrogen consumption and generation for December are 6048.131 gm mol and 9732.806 gm mol respectively and cumulative hydrogen consumption and generation for the month May is found to be 6173.209 gm mol and 16665.002 gm mol respectively.

The electrolyzer input is 246.258 kW which is obtained and taken at noon for May because May has the highest solar radiation and electrolyzer input will be maximum due to greater production of hydrogen by electrolyzer, hence electrolyzer which works well in May will work well throughout the year.

Equation 18 determines the hourly current required for a gas compressor. It is less for December than May due to less production of hydrogen in December thereby requiring less power to compress generated hydrogen during sunshine hours. The number of PV modules needed in parallel is calculated as 125 and calculated only for December as month December has minimum solar radiation and if module number in parallel needed is satisfied in December, the system will work throughout the year. The number of modules in series for the gas compressor is 2. The gas compressor rating at 48 V is found to be 24.542 kW and is taken from May at noon because at this time the hydrogen production is maximum (2050.132 gm.mol) and consumption of power by the gas compressor to compress large hydrogen generated by electrolyzer is maximum, Hence gas compressor if it works well in this time and it can work well also throughout the year.

Table 2 shows the ratings of different power system components.

Table 2: Ratings of power system components.

Components of power system	Rating
No. of photovoltaic modules in parallel(N_p)	1213
No. of photovoltaic modules in series(N_s)	2
Electrolyzer input at 48V	246.258 kW
No. of fuel cell in a stack($N_{fcseries}$)	47
No. of fuel cells stacks($N_{fcparallel}$)	36
Maximum output of each fuel cell stack	7.966A, 382.372 W
Gas compressor rating at 48V	24.542 kW
No. of photovoltaic modules in parallel for gas compressor($N_{p,compressor}$)	125
No. of photovoltaic modules in series for gas compressor($N_{s,compressor}$)	2

V. CONCLUSION

It can be stated that for operating water-LiBr VARS at evaporator cooling load of 10 TOR and temperatures of the evaporator, absorber, generator and condenser as 15⁰ C, ambient temperature(December, May), 80⁰C and ambient temperature(December, May) respectively, 1213 solar PV modules in parallel, 2 solar PV modules in series of Central Electronics Limited Make PM 150 with a 246.258 kW electrolyzer and 36 PEM fuel cell stacks, each of 382.372 W can support the working of VARS throughout the year. 125 solar photovoltaic modules in parallel each having 2 modules in a series of Central Electronics Limited Make PM 150 is needed to run the gas compressor for storing hydrogen in the cylinder during sunshine hours. In this work month, May and December are chosen as May has maximum solar radiation, maximum ambient temperature and December has minimum solar radiation, minimum ambient temperature for Kolkata city, India. Hence if the system works well in these two months the system will work well throughout the year. If the evaporator cooling load of VARS is increased, then the number of PV modules and capacity of the electrolyzer, fuel cell requirement will increase.

REFERENCES

- [1]. S.H.Wu, D.B.Kotak, and M.S.Fleetwood, An integrated system framework for fuel cell-based distributed green energy applications, *Renewable Energy*, 30, 2005, 1525-1540.
- [2]. A. Yildiz, O. Ozgener, and L. Ozgener, Exergetic performance assessment of solar photovoltaic cell (PV) assisted earth to air heat exchanger (EAHE) system for solar greenhouse cooling, *Energy and Buildings*, 43, 2011, 3154-3160.

- [3]. Y.Bai, G.Fraisse, F.Wurtz, A.Foggia, Y.Deless, and F.Domain, Experimental and numerical study of a directly PV-assisted domestic hot water system, *Solar Energy*, 85,2011,1979-1991.
- [4]. N. A.Kelly, T. L. Gibson, and D. B.Ouwerkerk,Generation of high-pressure hydrogen for fuel cell electric vehicles using photovoltaic-powered water electrolysis,*International Journal of Hydrogen Energy*,36,2011,15803-15825.
- [5]. I. Navarro-Solís, L. Villalba –Almendra, and A. Alvarez-Gallegos, H₂ production by PEM electrolysis, assisted by textile effluent treatment and a solar photovoltaic cell,*International Journal of Hydrogen Energy*,35,2010,10833-10841.
- [6]. V.Dorer, R. Weber, and A.Weber, Performance assessment of fuel cell micro-cogeneration systems for residential buildings, *Energy and Buildings*,37, 2005, 1132-1146.
- [7]. H. Tributsch, Review Photovoltaic hydrogen generation, *International Journal of Hydrogen Energy*,33,2008,5911-5930.
- [8]. J. Jie, L. Keliang, C. Tin-tai, P. Gang, H. Wei, and H. Hanfeng, Performance analysis of a photovoltaic heat pump, *Applied Energy*,85, 2008, 680-693.
- [9]. A.D.Hawkes, P.Aguier, C.A.Hernandez-Aramburo, M.A.Leach, N.P.Brandon, T.C.Green, and C.S.Adjiman, Techno-economic modelling of a solid oxide fuel cell stack for micro combined heat and power, *Journal of Power Sources*,156, 2006, 321-333.
- [10]. F.L. Lansing, Computer modelling of a single stage lithium bromide/water absorption refrigeration unit, *JPL Deep Space Network progress Report 42-32, DSN Engineering section*, 1976, 247-257.
- [11]. W. Wagner, J. R. Cooper, A. Dittmann, J. Kijima, H. J. Kretzschmar, and A. Kruse, The IAPWS Industrial Formulation 1997 for the thermodynamic properties of water and steam, *Journal of Engineering for Gas Turbines and Power*, 122,2000,150-182.
- [12]. J. Patek, and J. Klomfar, A computationally effective formulation of thermodynamic properties of LiBr–H₂O solutions from 273 to 500 K over full composition range, *International Journal of Refrigeration*,29, 2006, 566-578.
- [13]. Solar photovoltaic modules pm 150. <http://celindiacoin.preview1.cp247.net/cal/PM150.pdf>, 2011 (accessed on 1st November, 2011).
- [14]. K.Talukdar, Modeling and Analysis of Solar Photovoltaic Assisted Electrolyzer-Polymer Electrolyte Membrane Fuel Cell For Running a Hospital in Remote Area in Kolkata, India, *Int. Journal of Renewable Energy Development*,6 (2), 2017,181-191.
- [15]. Telecommunication Engineering Centre (TEC), New Delhi. Planning and maintenance guidelines for SPV power, 2011 (Accessed on 23rd March, 2011).
- [16]. S. K. Patra, and P. P. Datta, Some insights into solar photovoltaics-solar home lighting system, NABARD Technical Digest 7,<http://www.nabard.org>.(Accessed on 26.06.2009).
- [17]. N. V. Dale, M. D. Mann, and H. Salehfar, Semi-empirical model based on thermodynamic principles for determining 6 kW PEM electrolyzer stack characteristics, *Journal of Power Sources*, 185(2),2008,1348-1353.

Dr. Kamaljyoti Talukdar. "Modeling of vapour absorption refrigeration system assisted by solar photovoltaic and electrolyzer-polymer electrolyte membrane fuel cell." *IOSR Journal of Mechanical and Civil Engineering (IOSR-JMCE)*, 17(3), 2020, pp. 37-48.